On the horizontal variability of the upper ocean

Daniel L. Rudnick

Scripps Institution of Oceanography, La Jolla, California

Abstract. The last decade has seen a tremendous increase in the number and quality of observations of horizontal structure in the upper ocean. Many of these data have been made possible by the widespread use of towed vehicles and shipboard Doppler sonars. We review what these observations have revealed about processes in the upper ocean, with special emphasis on mid-latitudes and horizontal scales of 1-100 km. Fronts are one of the most prominent features of the mixed layer on these scales. The vertical/across-front circulation created at a front may be quantified assuming quasigeostrophic dynamics. Typical of the mixed layer are fronts that are warm and salty on one side, and cool and fresh on the other such that the density contrast across the front is small. The ubiquitous existence of such compensated fronts suggests that horizontal mixing in the mixed layer is an increasing function of the horizontal density gradient. Arguments based on the conservation of potential vorticity indicate that 10-km-scale (roughly the Rossby radius of deformation) eddies in the mixed layer should be predominantly cyclonic. Recent observations of mixed-layer vorticity are positively skewed.

Introduction

The database of small horizontal scale upper ocean observations has grown significantly in recent years due to the increased use of towed vehicles (such as SeaSoar), shipboard Acoustic Doppler Current Profiler (ADCP) and Global Positioning System (GPS) navigation. A brief review of these measurements is the purpose of this paper, with special emphasis on the mid-latitude open ocean on scales of 1-100 km.

Relevant characteristics of the instruments used in upper ocean surveying are as follows. SeaSoar is a towed vehicle capable of cycling from the surface to over 300 m every 3-4 km at a tow speed of 4 m s^{-1}. SeaSoar usually carries a CTD, providing measurements of temperature, salinity, and pressure. A 150-kHz ADCP in typical use allows horizontal resolution of velocity quite similar to that of a SeaSoar, with vertical coverage of 200-300 m. High quality GPS navigation is a key part of the surveying system, especially for retrieving the best absolute velocity. P-code receivers, in use on many research vessels, offer positional accuracy of about 3 m.

Observations are used to address three issues. (1) The anatomy of an upper ocean front is discussed, including the vertical/across-front circulation and associated heat flux. (2) Compensation of horizontal temperature and salinity gradients in the mixed layer is shown common. (3) Cyclonic vorticity is preferred at small horizontal scales in the mixed layer. For each of the above issues, we discuss what the observations suggest about mixing in the ocean.

The anatomy of an upper ocean front

The most common use of the SeaSoar/ADCP/GPS system has been to survey individual features in the upper ocean. Such a survey of the Azores Front in the North Atlantic, done in March 1992, demonstrates many phenomena common to oceanic fronts [*Rudnick and Luyten*, 1996]. The survey, consisting of a series of north/south sections separated by one-quarter of a degree in longitude, reveals a sharp density front (Figure 1). Horizontal velocity approaches 0.5 m s^{-1}, and is generally directed parallel to isopycnals. This intuitive result has two implications. First, surveying techniques are accurate enough that coherent velocity and density fields can be measured. Second, and more importantly, the rate of change and vertical advection of density must be small. The velocity field is in the form of a jet strongest at the density front. The jet, and its associated straining, causes streamers in the alongfront direction. Enhanced horizontal variability is typical of frontal regions [*Ferrari and Rudnick*, 2000].

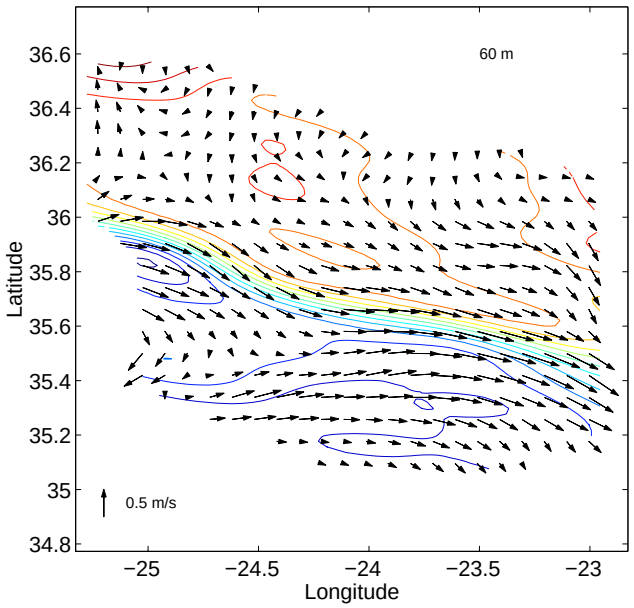

Figure 1. Potential density and horizontal velocity in the mixed layer at the Azores Front. The contour interval is 0.025 kg m^{-3}, and the velocity scale is shown. Note the jet directed along the density front.

The vertical/across-front structure is seen in a north/south section along 24.25°W (Figure 2). Mixed-layer depth trends from about 100 m deep in the northern part of the section to roughly 150 m in the south. The mixed-layer base is marked as a region of strong stratification. The front is apparent as isopycnals slope upward and to the north across the mixed layer. One can think of the structure almost as a piece of the mixed-layer base peeling off and intersecting the surface. Because the survey is from late winter, following a period of relative calm, restratification is just beginning. A shallow stratified layer lies over the mixed layer north of the front. Isopycnals retain a strong slope in the thermocline beneath the surface front. The Azores Front is, in fact, a permanent feature that penetrates to a depth of 2000 m [*Gould*, 1985]. There is some suggestion of subduction, as mixed-layer water from the north side of the front appears to slide southward and below the outcropping front.

The simplest dynamical balance one can imagine testing is thermal wind. Such a test is possible by comparing the independently measured fields of velocity shear and density (Figure 2). Strong shear of the correct sign is apparent along the outcropping isopycnals in the mixed layer, and downward and southward beneath the mixed layer. Alternating bands of positive and negative shear are apparent at the mixed layer base north of the front. These shears are clearly out of thermal wind balance, and are likely near-inertial.

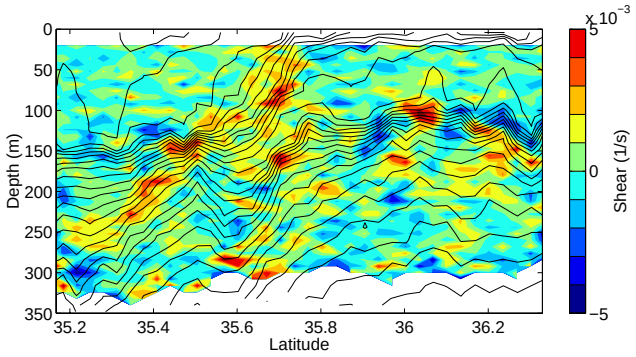

Figure 2. North/south section of potential density and vertical shear of velocity. The contour interval of density is 0.025 kg m^{-3}. Note the high shear along the sloping front.

The vertical velocity field may be inferred assuming quasi-geostrophic dynamics. This assumption is reasonable because the front is observed to be nearly in thermal wind balance. Derivation of the resulting omega equation [*Hoskins et al.*, 1978] relies on the elimination of the time derivative terms in the momentum and density equations. The omega equation can be written

$$\nabla^2\left(N^2 w\right) + f^2 \frac{\partial^2 w}{\partial z^2} = 2\nabla \cdot \mathbf{Q}\,, \qquad (1)$$

where

$$\mathbf{Q} = \frac{g}{\rho_0}\left(\frac{\partial \mathbf{u}_g}{\partial x}\cdot\nabla\rho, \frac{\partial \mathbf{u}_g}{\partial y}\cdot\nabla\rho\right), \qquad (2)$$

and $\mathbf{u}_g$ is geostrophic velocity, the divergence operator is two-dimensional and other symbols have their usual meaning. Forcing of the omega equation is a function of the density and geostrophic velocity fields.

The elliptic omega equation is solved for the survey of the Azores Front [*Rudnick*, 1996]. A band of downwelling exists near and to the north of the front (Figure 3). Upwelling appears on the south side of the front especially at about 24°W. A region of strong downwelling occurs in the SW corner where the flow is southward. The tendency for downwelling on the dense (cold) side of the front and upwelling on the less dense (warm) side results in a net heat flux averaged over the horizontal area of the survey. The heat flux peaks at the base of the mixed layer at about 15 W m^{-2}. This heat flux is comparable to, or larger than, climatological values compiled on 1° grids [*Marshall et al.*, 1993].

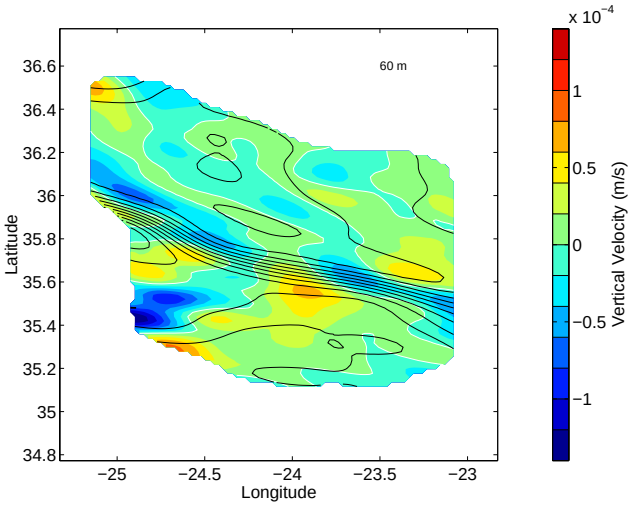

Figure 3. Vertical velocity and potential density in the mixed layer at the Azores Front. The contour interval for potential density is 0.025 kg m^{-3}. The white contour indicates zero vertical velocity. Note the band of downwelling in and to the north of the front.

A simple theory of a semi-geostrophic front [*Hoskins and Bretherton*, 1972] helps to understand the observations. The two-dimensional model relies on the assumption that the across-front momentum balance is exactly geostrophic, but the alongfront balance includes horizontal and vertical advection (see Appendix). The front is formed by a large-scale deformation of an initially vertically uniform layer with weak horizontal density gradients. The solution (Figure 4) is shown at time $4/\alpha$, where α is the rate of strain. The large-scale strain estimated from the velocity field of Figure 1 is approximately 10^{-6} s^{-1}, so the dimensional time would be 46 days. Sloping isopycnals

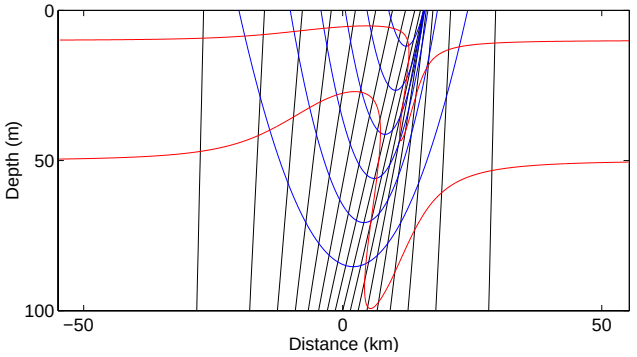

Figure 4. The semi-geostrophic model of frontogenesis at time $4/\alpha$. Black lines are isopycnals with a contour interval of 0.2 kg m^{-3}. Lines of constant along-front velocity (blue) have an interval of 0.1 m s^{-1}. The red lines show the positions of particles initially at 10 and 50 m.

are pinched at the surface forming a front. An essential feature of this model is that an infinitely sharp front is formed in a finite time. Alongfront velocity is in the form of a surface intensified jet with the dense (positive vorticity) side sharper than the light (negative vorticity) side. As the solution is Lagrangian, it is a simple matter to determine the position of particles. The initial 10 and 50 m surfaces have been stirred to be multi-valued as a function of horizontal position. Strong localized downwelling occurs on the dense side of the front with weaker, more diffuse, upwelling on the less dense side. This pattern of vertical velocity is consistent with the observations.

Temperature/salinity compensation

Mixed-layer thermohaline fronts are often observed to have a gradient from warm and salty to cool and fresh such that the density contrast across the front is small. This phenomenon is termed compensation because temperature and salinity compensate in their effects on density. Compensation has been known for some time at large and meso scales [*Roden*, 1975; *Roden*, 1984]. More recently, compensation has been shown to exist at horizontal scales as small as 10 m [*Ferrari and Rudnick*, 2000; *Rudnick and Ferrari*, 1999].

The existence of compensation in the mixed layer is consistent with theory proposed by Young [1994] and Ferrari and Young [1997]. Consider a vertically mixed layer with an initially random distribution of temperature and salinity. Temperature and salinity gradients compensate in their effect on density in some regions, while in others density gradients exist. Density gradients slump due to gravity, creating sloping isopycnals. Vertical mixing results in weakened horizontal density gradients. This process is essentially shear dispersion [*Taylor*, 1953] where the shear is due to slumping density gradients, and the mixing is caused by any of the processes that make the mixed layer vertically uniform. Temperature/salinity gradients that are compensated do not slump and therefore do not experience shear dispersion. The net effect is that density gradients diffuse while compensated gradients persist.

Compensation is manifest as a strong correlation between temperature and salinity in a horizontal SeaSoar tow in the N. Pacific winter mixed layer [*Ferrari et al.*, this volume]. Temperature and salinity fluctuations coincide at all resolved scales. The observations are thus consistent with a horizontal diffusivity that is an increasing function of horizontal density gradient.

An important question is under what conditions is compensation typical of the world's oceans. This question is addressed using SeaSoar data from the midlatitude, northern hemisphere Pacific, Atlantic, and Indian Oceans during all seasons [*Rudnick and Martin*, 2001]. The relevant

quantity is the density ratio R, defined as the ratio of the effect of a horizontal change of temperature on density divided by that of salinity on density. For a compensated thermohaline front, R=1.

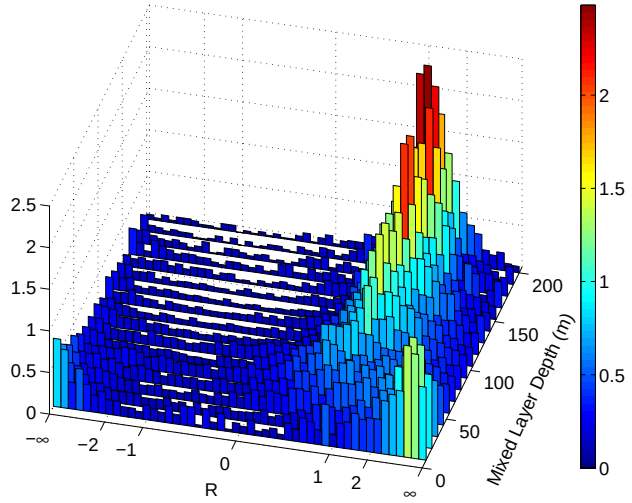

Figure 5. The conditional probability density function (pdf) of mixed-layer density ratio as a function of mixed-layer depth from the global ocean. Each row of bars represents the conditional pdf for the given mixed-layer depth. Height, and color shading, of the bars indicate the pdf magnitude. The density ratio is typically 1 for mixed layers deeper than 75 m.

The conditional probability density function (pdf) of mixed-layer density ratio as a function of mixed-layer depth summarizes results from the global ocean (Figure 5). For mixed-layers deeper than 75 m a density ratio near 1 is typical, while shallower mixed layers have a poorly defined density ratio. The shallowest mixed layers are temperature dominated as the density ratio approaches infinity. Mixed-layer depth may be considered a proxy for the strength of vertical mixing. The results suggest that vertical mixing is essential to the establishment of compensation in the mixed layer. This observation is consistent with the slumping and mixing model where vertical mixing is an essential process. On the other hand, compensation should not be expected in shallow mixed layers where vertical mixing is weak.

A density ratio of two is typical of the thermocline beneath the mixed layer [*Schmitt*, 1981]. This phenomenon is believed to be caused by salt fingering [*Schmitt*, 1994]. What is remarkable is the sharpness of the transition from R=1 to R=2 across the mixed-layer base, especially when the mixed layer is deep [*Ferrari and Rudnick*, 2000; *Rudnick and Martin*, 2001]. The change in density ratio from the mixed layer to the thermocline is a reflection of the different mixing processes working in the two regions.

Mixed-layer vorticity

Rapidly rotating vortices in the ocean are, in theory, predominantly cyclonic. A simple explanation invokes the conservation of potential vorticity as in the two-dimensional Hoskins and Bretherton semigeostrophic model (Figure 4). The potential vorticity for this model is

$$q = \frac{1}{\rho_0}\left[\frac{\partial \rho}{\partial z}\left(f + \frac{\partial v}{\partial x}\right) - \frac{\partial \rho}{\partial x}\frac{\partial v}{\partial z}\right]. \qquad (3)$$

The initial state of the model is one of zero q as the layer is vertically uniform and velocities are zero. As the front sharpens, gradients of density and velocity increase, but q must remain zero. Because of thermal wind, the second term above is always positive (in the northern hemisphere). To conserve q then, the first term must be negative. As static stability requires $\partial \rho / \partial z \le 0$, absolute vorticity must remain positive. If the relative vorticity is to be the magnitude of f or larger, it must thus be cyclonic.

The discussion above has relevance to the symmetric instability [*Hoskins*, 1974]. The symmetric instability considers an exactly circular vortex, so a two-dimensional model (radial/vertical) is sufficient. Instability occurs if the potential vorticity, given by (3), is positive. Hoskins points out that a statically stable, motionless state cannot evolve frictionally and adiabatically to a state subject to symmetric instability.

The relevant length scale in the ocean is the Rossby radius of deformation for the mixed layer, of order 10 km. The impediment to making accurate measurements of small-scale vorticity using shipboard ADCP data has been navigation. With the advent of military grade (P-code) GPS, this problem has been solved.

Vorticity is estimated using data of 3-km horizontal resolution from a cruise in the North Pacific during the winter of 1997 [*Rudnick*, 2001]. Because a SeaSoar was used, underway estimates of mixed-layer depth are available. The pdf of mixed-layer relative vorticity normalized by planetary vorticity has a mode near zero and is positively skewed (Figure 6). The skewness is apparent as a relatively thick tail at a normalized vorticity of 0.5. The skewness of vorticity is 0.36, and is considered statistically significant. The skewed vorticity is likely the velocity signature of spiral eddies seen in photographs of the sea surface [*Munk et al.*, 2000]. The contribution of these eddies to mixing in the ocean is an open question.

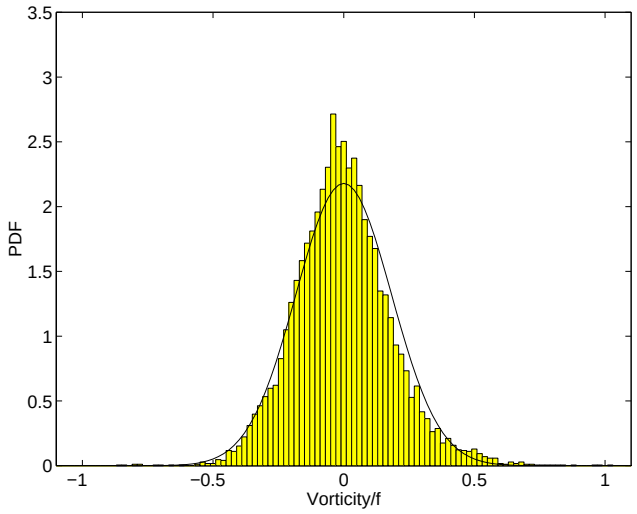

Figure 6. Probability density function (pdf) of relative vorticity normalized by planetary vorticity in the mixed layer. A normal distribution with zero mean and standard deviation, 0.18, equal to the observations is shown (solid line). The skewness, equal to 0.36, is apparent as the relatively high value of the pdf near a normalized vorticity of 0.5.

Summary

Shipboard surveys using SeaSoar and ADCP have greatly improved our knowledge of small-scale horizontal variability in the upper ocean. Oceanic fronts are observed to be in approximate thermal wind balance. A restratifying across-front circulation can be inferred, implying a heat flux of order 10 W m^{-2} when averaged over a 100 km^2 region surrounding the front. Temperature/salinity compensation is typical in the mixed layer, especially when the mixed layer is deep. The observed compensation is consistent with the slumping and mixing model of Young and colleagues, and a horizontal diffusivity that is a growing function of density gradient. Mixed-layer vorticity is skewed positive because the largest vorticities are positive. The observed skewness is consistent with potential vorticity conservation.

Appendix

The following is a review of the *Hoskins and Bretherton* [1972] two-dimensional semi-geostrophic model of frontogenesis. A novelty is that the solution is in fully Lagrangian coordinates, in contrast to the mixed Eulerian/Lagrangian solution in Hoskins and Bretherton.

The semi-geostrophic equations appropriate for a front in the x-direction are

$$-fv = -\frac{1}{\rho_0}\frac{\partial p}{\partial x} \tag{A1}$$

$$\frac{Dv}{Dt} + fu = -\frac{1}{\rho_0}\frac{\partial p}{\partial y} \tag{A2}$$

$$0 = -\frac{\partial p}{\partial z} - \rho g \tag{A3}$$

$$\frac{D\rho}{Dt} = 0 \tag{A4}$$

$$\frac{\partial u}{\partial x} + \frac{\partial v}{\partial y} + \frac{\partial w}{\partial z} = 0 \tag{A5}$$

where

$$\frac{D}{Dt} = \frac{\partial}{\partial t} + u\frac{\partial}{\partial x} + v\frac{\partial}{\partial y} + w\frac{\partial}{\partial z}.$$

Here, y is the along-front direction, z is vertical, ρ_0 is a constant reference density, and f is a constant Coriolis parameter. Ertel's potential vorticity (3) is conserved following fluid particles

$$\frac{Dq}{Dt} = 0 \tag{A6}$$

Assume a solution consisting of a geostrophic confluent flow plus a two-dimensional component,

$$u = -\alpha x + u'(x,z,t) \tag{A7}$$

$$v = \alpha y + v'(x,z,t) \tag{A8}$$

$$\frac{p}{\rho_0} = f\alpha xy - \left(\alpha^2 + \frac{d\alpha}{dt}\right)\frac{y^2}{2} + \frac{p'}{\rho_0}(x,z,t) \tag{A9}$$

$$\rho = \rho(x,z,t) \tag{A10}$$

$$w = w(x,z,t). \tag{A11}$$

Note that the parameter α may be a function of time.

Substitution of (A7-11) into (A1-5) yields the equations

$$\frac{DM}{Dt} + \alpha M = 0 \tag{A12}$$

$$\frac{\partial u}{\partial x} + \frac{\partial w}{\partial z} = -\alpha \tag{A13}$$

$$f\frac{\partial v'}{\partial z} = -\frac{g}{\rho_0}\frac{\partial \rho}{\partial x}, \tag{A14}$$

where

$$M = v' + fx.$$

These together with conservation of density (A4) are the equations we need to solve.

The prognostic equations (A12) and (A4) can be solved immediately in Lagrangian coordinates, with no explicit dependence on along-front position,

$$M = M_0(x_0, z_0)e^{-\beta} \tag{A15}$$

$$\rho = \rho(x_0, z_0), \tag{A16}$$

where

$$\beta(t) = \int_0^t \alpha(t')dt',$$

and x_0 and z_0 are the initial across-front and vertical positions of particles.

A useful identity expresses the Eulerian spatial gradient of a dependent variable h in Lagrangian coordinates,

$$\left(\frac{\partial h}{\partial x}\right)_z = \frac{\partial(h,z)}{\partial(x_0,z_0)}\left[\frac{\partial(x,z)}{\partial(x_0,z_0)}\right]^{-1}. \tag{A17}$$

where the subscript z on the lhs makes clear that z is held constant. Using (A17), (A13-14) can be written in Lagrangian coordinates as

$$\frac{\partial(x,z)}{\partial(x_0,z_0)} = e^{-\beta} \tag{A18}$$

$$f\frac{\partial(x,M)}{\partial(x_0,z_0)} = -\frac{g}{\rho_0}\frac{\partial(\rho,z)}{\partial(x_0,z_0)}. \tag{A19}$$

The solution in Lagrangian coordinates (A15-16) is simple. The challenge is the transformation back to Eulerian coordinates (A18-19). These equations are nonlinear, and possibly difficult to solve depending on the initial and boundary conditions used.

Potential vorticity may be written

$$q = \frac{1}{\rho_0}\frac{\partial(M,\rho)}{\partial(x,z)} = \frac{1}{\rho_0}\frac{\partial(M_0,\rho)}{\partial(x_0,z_0)}, \tag{A20}$$

and is necessarily conserved, as can be readily seen by its expression in Lagrangian coordinates.

Consider a layer initially vertically uniform in density. Suppose also that the initial horizontal density gradient is so small that along-front velocity and its vertical shear are negligible. Using these initial conditions, solutions are

$$M = fx_0e^{-\beta} \tag{A21}$$

$$\rho = \rho(x_0). \tag{A22}$$

Substituting these into the thermal wind equation (A19) and integrating yields

$$x = z\frac{g}{f^2\rho_0}\frac{\partial\rho}{\partial x_0}e^{\beta} + A(x_0,t), \tag{A23}$$

where $A(x_0,t)$ is to be determined from boundary conditions. Derivatives of x with respect to x_0 and z_0 can be derived from (A23) and substituted into the continuity equation (A18). Integrating the result with respect to z_0 gives

$$z\frac{\partial A}{\partial x_0} + z^2\frac{g}{2f^2\rho_0}\frac{\partial^2\rho}{\partial x_0^2}e^{\beta} = z_0e^{-\beta} + B(x_0,t). \tag{A24}$$

We use boundary conditions that particles on the top and bottom boundaries remain there

$$z(z_0 = \pm H) = \pm H. \tag{A25}$$

Evaluating (A24) at the boundaries, and using (A23), yields expressions for the integration constants

$$A = x_0e^{-\beta} \tag{A26}$$

$$B = H^2\frac{g}{2f^2\rho_0}\frac{\partial^2\rho}{\partial x_0^2}e^{\beta}. \tag{A27}$$

The solutions for x and z are thus

$$x = x_0e^{-\beta} + z\frac{g}{f^2\rho_0}\frac{\partial\rho}{\partial x_0}e^{\beta} \tag{A28}$$

$$z - z_0 + \left(z^2 - H^2\right)\frac{g}{2f^2\rho_0}\frac{\partial^2\rho}{\partial x_0^2}e^{2\beta} = 0. \tag{A29}$$

The solution in Figure 4 has an initial density profile that is an arctan with a length scale of 500 km, in a layer 200 m deep.

A few features of the solution are worthy of note. The absolute vorticity is

$$\frac{\partial M}{\partial x} = f\left[1 + z\frac{g}{f^2\rho_0}\frac{\partial^2\rho}{\partial x_0^2}e^{2\beta}\right]^{-1}. \tag{A30}$$

Vorticity becomes infinite in a finite time, provided the initial density profile has nonzero curvature. This will happen first on the boundaries.

The slope of an isopycnal,

$$\left(\frac{\partial x}{\partial z}\right)_{x_0} = \frac{g}{f^2\rho_0}\frac{\partial\rho}{\partial x_0}e^{\beta}, \tag{A31}$$

depends only on x_0 and t, so the isopycnal is a straight line.

The Richardson number is given by

$$Ri = \frac{N^2}{(\partial v/\partial z)^2} = \frac{f}{\partial M/\partial x}. \tag{A32}$$

Therefore, (A30) implies that Ri becomes zero in a finite time in the region of strong vorticity and subduction at the

front. *Ri* is 1 elsewhere. Mixing must become important as the front sharpens.

Acknowledgments. This paper reviews observations from several experiments over the last fifteen years. I thank the many PIs who are responsible for making these experiments successful. The Office of Naval Research and the National Science Foundation provided the funding for most of the work reviewed here. During the preparation of this paper, I was supported by NSF under grant OCE98-19521.

References

Ferrari, R., and D. L. Rudnick, Thermohaline variability in the upper ocean, *J. Geophys. Res.*, *105,* 16,857-16,883, 2000.

Ferrari, R., and W. R. Young, On the development of thermohaline correlations as a result of nonlinear diffusive parameterizations, *J. Mar. Res.*,
55, 1069-1101, 1997.

Gould, W. J., Physical oceanography of the Azores front, *Prog. Oceanog.*, *14,* 167-190, 1985.

Hoskins, B. J., The role of potential vorticity in symmetric stability and instability, *Quart. J. Roy. Meteor. Soc.*, *100,* 480-482, 1974.

Hoskins, B. J., and F. P. Bretherton, Atmospheric frontogenesis models: mathematical formulation and solution, *J. Atmos. Sci.*, *29,* 11-37, 1972.

Hoskins, B. J., I. Draghici, and H. C. Davies, A new look at the ω-equation, *Quart. J. R. Met. Soc.*, *104,* 31-38, 1978.

Marshall, J. C., A. F. G. Nurser, and R. G. Williams, Inferring the subduction rate and period over the North Atlantic, *J. Phys. Oceanogr.*, *23,* 1315-1329, 1993.

Munk, W., L. Armi, K. Fischer, and F. Zachariasen, Spirals on the sea, *Proc. R. Soc. Lond. A*, *456,* 1217-1280, 2000.

Roden, G. I., On North Pacific temperature, salinity, sound velocity and density fronts and their relation to the wind and energy flux fields, *J. Phys. Oceanogr.*, *5,* 557-571, 1975.

Roden, G. I., Mesoscale oceanic fronts of the North Pacific, *Ann. Geophys.*, *2,* 399-410, 1984.

Rudnick, D. L., Intensive surveys of the Azores Front, 2, Inferring the geostrophic and vertical velocity fields, *J. Geophys. Res.*, *101,* 16,291-16,303, 1996.

Rudnick, D. L., On the skewness of vorticity in the upper ocean, *Geophys. Res. Lett.*, *in press*, 2001.

Rudnick, D. L., and R. Ferrari, Compensation of horizontal temperature and salinity gradients in the ocean mixed layer, *Science*, *283,* 526-529, 1999.

Rudnick, D. L., and J. R. Luyten, Intensive surveys of the Azores Front, 1, Tracers and dynamics, *J. Geophys. Res.*, *101,* 923-939, 1996.

Rudnick, D. L., and J. Martin, P., On the horizontal density ratio in the upper ocean, *Dyn. Atmos. Oceans*, *in press*, 2001.

Schmitt, R. W., Form of the temperature-salinity relationship in the central water: Evidence for double-diffusive mixing, *J. Phys. Oceanogr.*, *11,* 1015-1026, 1981.

Schmitt, R. W., Double diffusion in oceanography, *Ann. Rev. Fluid Mech.*, *26,* 255-285, 1994.

Taylor, G. I., Dispersion of soluble matter in solvent flowing slowly through a tube, *Proc. R. Soc. Lond. A*, *219,* 186-203, 1953.

Young, W. R., The subinertial mixed layer approximation, *J. Phys. Oceanogr.*, *24,* 1812-1826, 1994.